2011

Scanning Capacitance Spectroscopy on n$^+$-p Asymmetrical Junctions in Multicrystalline Si Solar Cells

Chun-Sheng Jiang
National Renewable Energy Laboratory

Jennifer T. Heath
Linfield College

Helio R. Moutinho
National Renewable Energy Laboratory

Mowafak M. Al-Jassim
National Renewable Energy Laboratory

C.-S. Jiang, J. T. Heath, H. R. Moutinho, and M. M. Al-Jassim

Related Articles

Additional information on J. Appl. Phys.

Scanning capacitance spectroscopy on n^+-p asymmetrical junctions in multicrystalline Si solar cells

C.-S. Jiang,[1,a)] J. T. Heath,[1,2] H. R. Moutinho,[1] and M. M. Al-Jassim[1]

[1]*National Renewable Energy Laboratory, 1617 Cole Blvd. Golden, Colorado 80401, USA*
[2]*Linfield College, McMinnville, Oregon 97128, USA*

We report on a scanning capacitance spectroscopy (SCS) study on the n^+-p junction of multicrystalline silicon solar cells. We found that the spectra taken at space intervals of ~10 nm exhibit characteristic features that depend strongly on the location relative to the junction. The capacitance-voltage spectra exhibit a local minimum capacitance value at the electrical junction, which allows the junction to be identified with ~10-nm resolution. The spectra also show complicated transitions from the junction to the n-region with two local capacitance minima on the capacitance-voltage curves; similar spectra to that have not been previously reported in the literature. These distinctive spectra are due to uneven carrier-flow from both the n- and p-sides. Our results contribute significantly to the SCS study on asymmetrical junctions. © *2011 American Institute of Physics*. [doi:10.1063/1.3605507]

I. INTRODUCTION

Scanning capacitance microscopy (SCM) has been developed as a valuable nm-characterization technique for two-dimensional (2D) carrier mapping in semiconductor devices. The relative free carrier distribution has been successfully mapped with SCM in unipolar Si, and these maps yield absolute concentrations after calibration by another quantitative method in at least one sample location.[1] However, carrier extraction near an asymmetrical n^+-p or p^+-n junction and delineation of the junctions continues to be a challenge.

In an SCM measurement, the SCM tip, surface oxide, and sample surface form a metal-oxide-semiconductor structure. A DC bias is applied between the probe and the sample, V_s, and an additional AC bias allows the SCM signal dC/dV to be measured using a lock-in amplifier. Ideally, the SCM image is collected using the value of V_s that maximizes the SCM signal, dC/dV, indicating a flat-band condition at the surface. The electrical junction (EJ) is then assigned to the location at which the SCM signal crosses zero, $dC/dV = 0$, as it changes from positive (p-type) to negative (n-type). However, because the value of V_s yielding a flat-band condition is, in general, different between the p- and n-regions of the device, and because the capacitance response near the junction is complicated by the low carrier density in the junction depletion region, the apparent EJ location, as determined by $dC/dV = 0$, depends on the value of V_s and has an error of $\pm W$, where W is the junction depletion width.[1–4] For a narrow junction in a field-effect transistor, W is similar to the SCM probe size, a few tens of nm. However, for low-doped n^+-p junctions, such as those in crystalline Si (c-Si) solar cells, W is typically a few hundred nm, and a more complete understanding of the SCM signal in the vicinity of the junction is desirable for characterizing these devices.

An empirical determination of the C-V response near the junction depletion region, due to the super-low carrier concentration, has been discussed in the literature.[5] A more quantitative and sophisticated analysis combines inverse modeling and forward simulation to extract the carrier concentration from the SCM data and subsequently determine the junction locations, although this approach presumes a Gaussian doping profiling and flat density of state for the interface and oxide charges.[6]

Scanning capacitance spectroscopy (SCS), a measurement of SCM dC/dV as a function of V_s at designated locations in the SCM image, provides a richer characterization of the sample response.[4,5,7,8] In unipolar regions, the sign of dC/dV does not depend on V_s and is positive for p-type material and negative for n-type. The dC/dV-V_s spectra show a single peak at the flat-band voltage. When the probe is positioned in the junction area, the spectra consist of a peak and a valley with opposite signs, like a mixture of the two unipolar spectra, corresponding to U-shaped capacitance-voltage (C-V_s) curves. These low-frequency-like C-V_s curves are due to the intermittent flow of minority carriers from the other side of the junction depending on V_s. The tip screening length is greatly enhanced in the depletion region, and an overlapping response from the p and n regions occurs.[8] A qualitative model was proposed for a heavy-asymmetrical junction, where the light-doping is more dominant over the spectra than the heavy-doping and the C-V_s spectra show the characteristic U-shape from the EJ to metallurgical junction (MJ).[5]

In this paper, we discuss SCS spectra from asymmetrical n^+-p junctions. The low background doping (3.8×10^{16} cm^{-3}) provides a large depletion width ($W = 260$ nm) and thus allow us to investigate the fine spectral features and spectra transitions in the junction area. We focus on the spectra at closely spaced locations in the junction area and on the

a)Author to whom correspondence should be addressed. Electronic mail: chun.sheng.jiang@nrel.gov.

accuracy and resolution with which the junction is determined. Spectra taken at intervals spaced much more closely than the junction depletion width have not been discussed previously in the literature. We found that the characteristic spectra depend strongly on the location relative to the junction, and our results contribute significantly to the SCS/SCM study on the asymmetrical junctions.

II. EXPERIMENTAL

The devices were typical multicrystalline Si (mc-Si) solar cells with grain sizes in the centimeter scale, which were created by phosphorus diffusion into mc-Si wafers. One typical doping profile of the devices, with which the SCM/SCS results are shown in this paper, is shown in Fig. 1, as measured by secondary ion mass spectrometry (SIMS). The doping profile and concentration are uniform across the 6 in. cell. The SIMS data indicate a MJ depth of $x_m = 455 \pm 10$ nm from the SiN_x/Si interface. The built-in potential and carrier concentrations were simulated using the PC1D software[9] and the SIMS dopant profile, allowing the EJ location, $x_e = 480 \pm 10$ nm, to be identified.

To prepare the SCM cross-sectional sample, two cleaved pieces of a mc-Si device were glued front contact to front-contact with conducting epoxy, and the cross-section was chemical-mechanically polished (CMP) flat to nm order using a series of diamond pads and, finally, colloidal silica. The sandwich structure protects the SCM probe from dropping off of the sample edge during imaging, since the area around the device front surface is the focus of this study. The gluing and subsequent polishing were carried out carefully to avoid shunting the device, because many unexpected defects created during the polishing, such as particles and contaminations, can cause shunting the device. Gently pushing the sample against the diamond pad with a small controlled force and using clean and fresh pads was found to help avoid the shunting. A post-anneal treatment for 30 mins at 300 °C under ultraviolet illumination significantly improved the SCM signal quality, indicating a less defective surface oxide.[1,5]
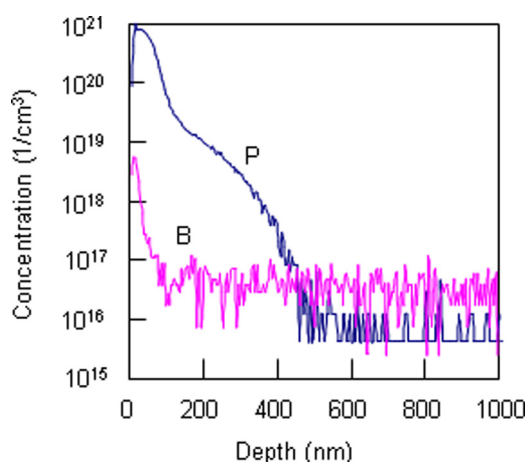
The SCM/SCS data were collected with the Veeco D3100 atomic force microscope (AFM) equipped with the Nanoscope V controller. Pt-Ir coated Si tips with a low spring constant ~0.2 nN/m were used in the contact mode of the AFM. This system uses an RCA capacitance sensor with UHF frequency of ~1 GHz, mounted in the vicinity of the AFM tip and connected to the tip using a short wire to minimize the stray capacitance. The DC voltage was $V_s = -1$ V for the SCM images shown here, and the AC voltage amplitude was 1 V for SCM and SCS measurements. These voltages were applied to the sample, and the tip remained at virtual ground.

The front and back contacts of the live device were connected to avoid photovoltage generation by the AFM laser ($\lambda = 670$ nm). Indeed, when the laser was turned off using the "dark lift" mode, we did not observe any measureable affect on the SCM images, which is different from the literature[10,11] and is likely a result of a different sample setup. Intentionally connecting the contacts of a live device so that every local area of the front and back contacts are shorted could result in a different sample condition from an unintentionally, and unevenly, shorted device.

For the SCS measurement, V_s was swept at 2 Hz with 256 steps in -3 — $+2$ V, which is fast enough to suppress the thermal drift and slow enough to suppress the spectra hysteresis. For well-prepared samples with minimum oxide and interface states/charges, reliable spectra with good signal quality and small hysteresis can be acquired with a few Hz scan rate; an example of the spectra taken in the forward and backward V_s scans on the p-side of the junction is shown in Fig. 2. Nevertheless, we take the average of the dC/dV-V_s spectra. After an SCM image was taken, the SCS were taken pixel by pixel along a designated line across the center of the image with a step of ~12 nm and a total of 100 pixels. To maintain accurate control of the tip location while SCS data were taken, the closed-loop control of the lateral scan was used, and the thermal drift was further suppressed by waiting for several hours before the measurements. After the SCS data were collected, a follow-up SCM image was taken to

FIG. 1. (Color online) SIMS P- and B-doping profiles measured on the mc-Si solar cell.
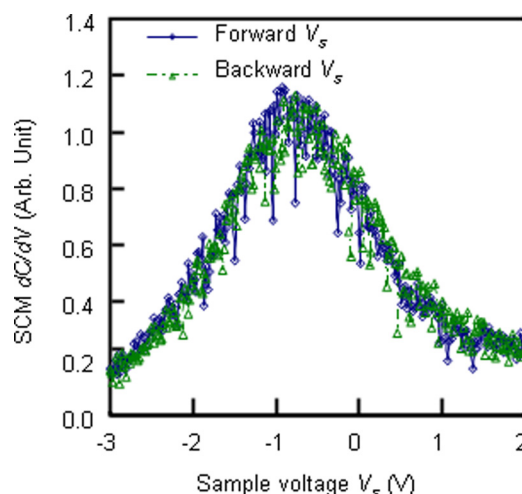

FIG. 2. (Color online) Example spectra taken in forward and backward V_s scans on the p-side of the junction, illustrating the SCM signal quality and small hysteresis of a reliable spectra measurement.

confirm the coincidence of the image location and to confirm the absence of any surface damage caused by the DC bias. For the SCS data presented here, we did not observe any measureable drift or change of the SCM images. Together with the careful scanner calibration, we believe that the SCS positions are highly accurate.

III. RESULTS AND DISCUSSIONS

Figure 3 shows a typical SCM image taken on the mc-Si solar cells with a diffused junction, the doping profile of which is shown in Fig. 1. The dC/dV profile was averaged over the 24 lines of the image, and the built-in potential and carrier concentrations were calculated by the PC1D simulation and the doping profile. The location corresponding to $dC/dV = 0$ is ~170 nm and ~190 nm shallower than the MJ and the EJ, respectively, and is not suitable for identifying the junction location. However, a "plateau" with a slower change is seen in the junction area.[5] In order to better understand the SCM image, we focus on the SCS spectra around the junction area. We will first show the overall spectra at the characteristic locations, labeled by pixel number in Fig. 3, and then concentrate on the junction area to explore possible junction identification criteria.

Six spectra are displayed in Fig. 4, which correspond to a location deep in the p-region (pixel #14), the location of maximum SCM signal (#41) in the p-depletion region, the EJ (#48), the MJ (#50), the location of minimum SCM signal (#68), and a shallow location in the n-region (#77). The C-V_s spectra are obtained by numerical integration from the dC/dV-V_s spectra. The spectra in the p-region (#14 and #41) are nearly identical, showing the typical p-type doping signature with $dC/dV > 0$ for the full range of V_s. These spectra can be fit to a Gaussian like curve centered around $V_{cp} = -0.56$ V and with half width $\sigma_p = 0.9$ V, as shown by the solid line in the figure.[4,5,7,8]

As the tip nears the EJ location and moves into the n region, the spectra change significantly. At the EJ (#48), the

FIG. 4. (Color) (a) The SCS spectra, dC/dV-V_s, and (b) the corresponding C-V_s spectra taken in a location deep in the bulk (#14), the maximum dC/dV location (#41), the EJ (#48), the MJ (#50), the minimum dC/dV location (#68), and a shallow location in the n-region (#77). All the locations are indicated in Fig. 3. All the symbols in (a) are the spectra data. The three solid curves are Gaussian fitting to the data at #14 and #68, and a composed curve from the Gaussian curves, which is observed matching the spectra at #48.

dC/dV spectrum contains strong negative and positive contributions. As the tip moves to the MJ (#50) and onward toward the bulk n-region, the spectrum gradually changes to n-type. This negative-going peak is broader than that seen in the p-region and is shifted to lower values of V_s. It can be fit by a Gaussian like curve centered around $V_{cn} = -2.0$ V and with half width $\sigma_n = 1.45$ V. We observe a smaller valley, corresponding to the higher doping concentration, at #77 than at #68.

Both the SCS peak height and width are larger in the p-region due to the lower p-type doping. Within the depletion region, asymmetrical spectra result from the uneven charge flow from the two sides of the junction, due to the respective charge screening lengths and carrier overlapping.[4,8] At the EJ location, the spectrum is fit well by a sum of the typical n- and p- Gaussian like curves, with equal magnitudes. The influence of the p-signature persists well within the n-region, 125 nm beyond the n-depletion edge. We believe that this is due to the screening length for the tip bias, which, if it extends into the junction depletion region, will cause a response from the p-side of the device.

Having discussed the overall characteristics of the spectra, we next focus on SCS data from pixels very near to the
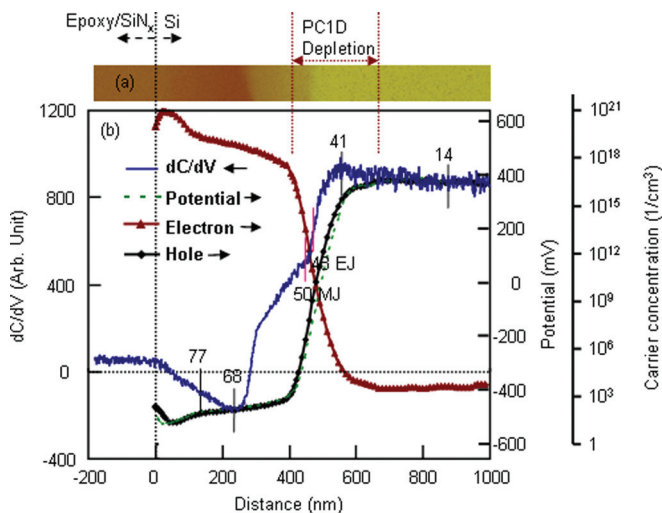

FIG. 3. (Color) (a) A slice of SCM dC/dV image measured on the junction area of the mc-Si solar cell. (b) shows the averaged dC/dV profile and the calculated carrier concentrations and built-in potential. The short vertical lines indicate the characteristic locations where the SCS spectra are shown in Fig. 4. The numbers present the SCS pixel number.
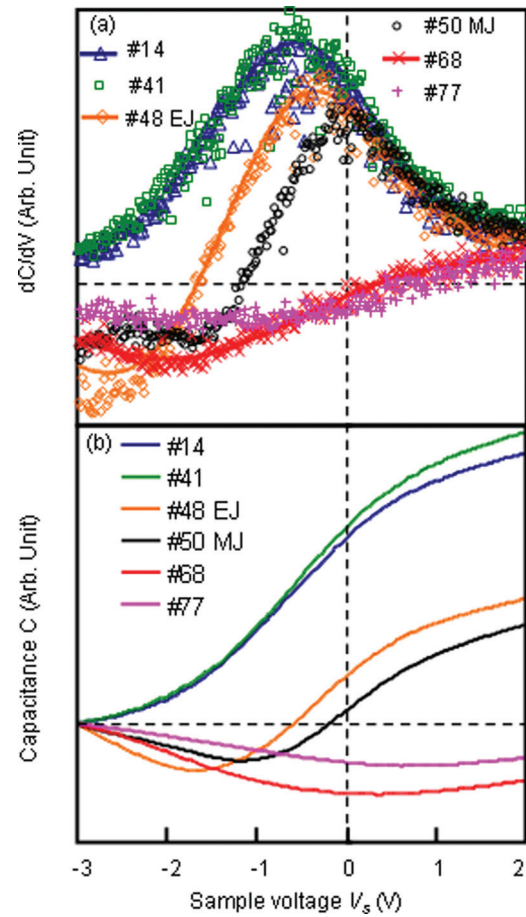
junction location. The spectra in the junction area are displayed below, pixel by pixel. Fig. 5 illustrates the locations at which spectra were collected, compared to the SIMS MJ and simulated EJ locations, and Fig. 6 shows the corresponding spectra. The spectra exhibit clear characteristics. With the tip approaching the EJ (#46-#48), the negative portion of the dC/dV-V_s spectrum becomes more dominant and extends over a larger range of V_s. These changes result in deeper valleys in the C-V_s curves. The most negative dC/dV value and the deepest C-V_s valley are observed at the EJ (#48). On the n side of the EJ, the onset of negative dC/dV-V_s continues to occur at progressively larger values of V_s. However, since the dC/dV values within the negative range remain relatively-flat, the C-V_s valley is less deep.

   With the tip away from the EJ and MJ and entering the n-region (#51), an additional local minimum at $V_s \sim -1.5$ V and a maximum at $V_s \sim -2.2$ V appear. When the local maximum is positive, this causes the C-V_s curve to change to a W-shape. This unusual spectral feature persists over a range of 80 nm, extending past the n-depletion edge and into the bulk n-region.

   The spectra in this transition region are complicated; similar spectra have not been reported both experimentally and numerically. Although the physical origin is now unclear, it is likely related to the characteristic one-sided doping profile in the solar cell devices, including the gradient in n^+ doping due to the diffused junction. A double-peak shape can be obtained from a simple sum of two Gaussians; however, a reasonable fit to these spectra would require a smaller σ_n and V_{cn} than are observed in the bulk region. Therefore, uneven carrier flows from both p- and n-sides are possibly a mechanism for these spectral features, and the factors describing the degree of the uneven flow should depend strongly on the location relative to the junction and on the doping profile in the n-region. A three-dimensional modeling using the doping profile is expected to quantitatively understand these characteristic spectra.

   The distinctive features at the EJ, including equally weighted contributions from the n- and p-type signals and

FIG. 6. (Color) (a) The SCS spectra, dC/dV-V_s, and (b) the corresponding C-V_s spectra taken around the junction area, shown pixel by pixel. The C-V_s spectra are shown in the negative C and V_s ranges to zoom-in the fine spectral features.
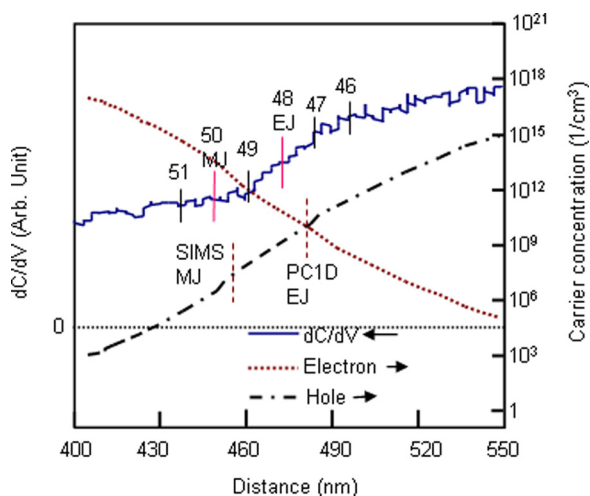
FIG. 5. (Color online) A zoom-in of Fig. 3 around the junction area. Vertical solid lines indicate the locations where the spectra are shown in Fig. 6. The vertical red dashed lines indicate the SIMS MJ and simulated EJ.
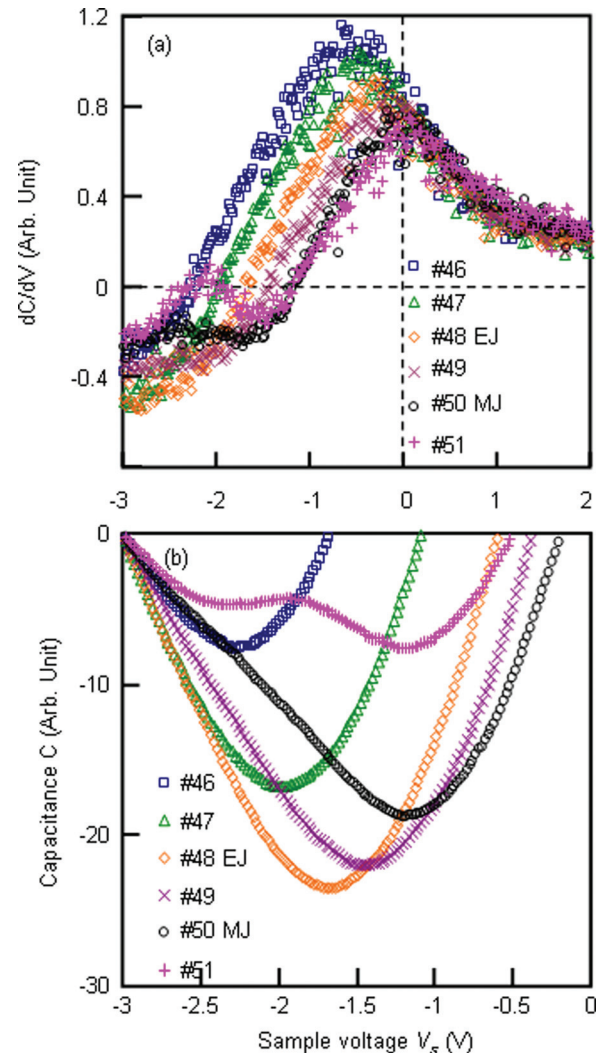
the deepest C-V_s valley, can be used for identifying its location, $x_e = 472$ nm. The SCS spectra within the depletion region change rapidly with tip position, allowing the EJ to be clearly distinguished from neighboring pixels, where the step between the pixels is 12 nm. Therefore, we believe that the resolution of the junction identifications is in the 10 nm range. This compares favorably to the EJ location identified with a combination of SIMS measurement and PC1D simulation, at $x_e = 480 \pm 10$ nm. The tip apex radius ($\sim$30 nm) is significantly larger than the spectral resolution. This is not surprising because the spectra are determined by the charge flow from both n- and p-sides and the magnitudes of the flow possibly change sensitive enough around the EJ to ensure the fine spectral resolution.

   With the tip location shallower than $x < 285$ nm (#64), which is $\sim$170 nm shallower than the MJ and $\sim$125 nm shallower than the n-depletion edge, the dC/dV spectra exhibit the typical n-signature: a smaller negative valley with higher doping concentration, as discussed above. It is necessary to show how the spectra transit from the W-shape to the n-signature ($x = 433$-285 nm). Figure 7 displays the spectra from
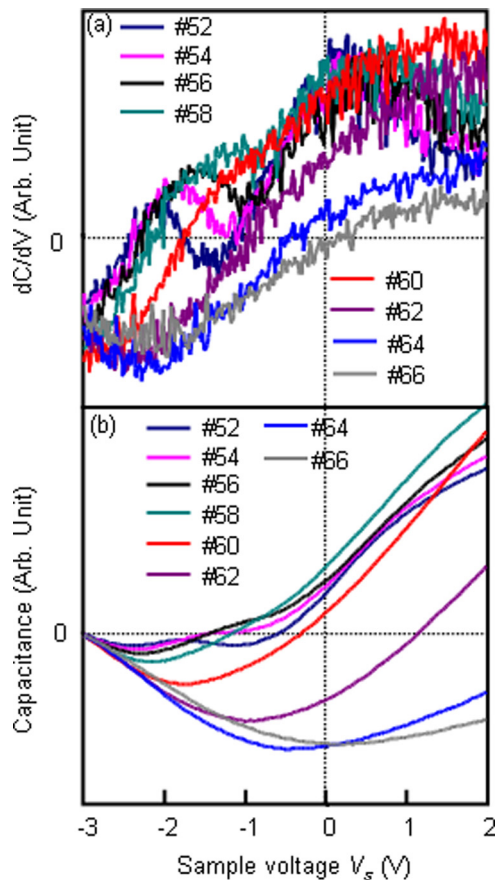
FIG. 7. (Color) (a) The SCS spectra, dC/dV-V_s and (b) the corresponding C-V_s spectra taken in the spectral transition region from $x = 425$ nm to $x = 262$ nm (#52-#66). The spectra in this region show first the W-shaped C-V_s curves and then U-shaped curves with a deeper valley at a larger doping location that is opposite to the typical n-signature.

#52 ($x = 425$ nm) to #66 ($x = 262$ nm). The spectra in this transition are complicated; similar spectra have not been reported in the literature.[1,4,5,7,8] The transit first exhibits the two local dC/dV maxima and minima and the W-shaped C-V_s curves in #51-#58 ($x = 433$—355 nm), then the single negative dC/dV valleys and the U-shaped C-V_s curves in #58-#64 ($x = 355$-285 nm). However, the spectra in this location range ($x = 355$-285 nm) is different from the typical n-doping, showing a larger negative dC/dV and a deeper C-V_s valley with a larger n-doping, which is opposite to the typical n-doping trend. Therefore, the affect from the p-side persists until $x = 285$ nm (#64). Locations shallower than this are screened completely from the charge flow from the p-side in the SCS measurement.

The spectral features discussed in this paper are commonly observed in the mc-Si cells with diffused junctions. The various grain orientations in the cells did not show significant difference in the spectral features, implying the uniform doping and uniform passivation of the surface and interface states and defects. With other solar cell devices, such as GaAs, different characteristic spectra were observed due to the different tip/sample contact and the sample electrical properties, which is not in the scope of this paper.

IV. CONCLUSION

We have achieved the measurement of SCS spectra in the junction area with closely spaced intervals by precisely positioning the tip and stabilizing the measurement conditions. The spectra taken on this asymmetrical junction of the diffused solar cell devices show much richer features and more complicated spectral transitions than what have been reported so far in the literature. The spectral features here depend strongly on the location relative to the junction, changed sensitively enough around the junction to ensure the EJ to be identified in ~10-nm resolution. The minimum capacitance value or the deepest valley on the C-V_s curves allows the EJ location to be delineated clearly. The spectra in the n-region right next to the MJ show anomalous W-shaped C-V_s curves. All these spectral features are likely due to the uneven charge flow from both the n- and p-sides and the characteristic doping profile in the diffused solar cell. Further quantitative modeling using the doping profile is expected to better understand the spectra.

[1]For a review, see C. C. Williams, Annu. Rev. Mater. Sci. **29**, 471 (1999).
[2]C. J. Kang, C. K. Kim, J. D. Lera, Y. Kuk, K. M. Mang, J. G. Lee, K. S. Suh, and C. C. Williams, Appl. Phys. Lett. **71**, 1546 (1997).
[3]M. L. O'Malley, G. L. Timp, S. V. Moccio, J. P. Garno, and R. N. Kleiman, Appl. Phys. Lett. **74**, 272 (1999).
[4]M. Stangoni, M. Ciappa, and W. Fichter, J. Vac. Sci. Technol. **B22**, 406 (2004).
[5]V. V. Zavyalov, J. S. McMurray, and C. C. Williams, J. Appl. Phys. **85**, 7774 (1999).
[6]W. K. Chim, K. M. Wong, Y. L. Teo, Y. Lei, and Y. T. Yeow, Appl. Phys. Lett. **80**, 4837 (2002).
[7]H. Edwards, R. McGlothlin, R. S. Martin, E. U. M. Gribelyuk, R. Mahaffy, C. K. Shih, R. S. List, and V. A. Ukraintsev, Appl. Phys. Lett. **72**, 698 (1998).
[8]M. L. O'Malley, G. L. Timp, W. Timp, S. V. Moccio, J. P. Garno, and R. N. Kleiman, Appl. Phys. Lett. **74**, 3672 (1999).
[9]PC1D version 5.3, ARC Photovoltaic Center of Excellence, University of New South Wales, Sydney, Australia, 1998.
[10]M. N. Chang, C. Y. Chen, F. M. Pan, J. H. Lai, W. W. Wan, and J. H. Liang, Appl. Phys. Lett. **82**, 3955 (2003).
[11]G. H. Buh, J. J. Kopanski, J. F. Marchiando, A. G. Birdwell, and Y. Kuk, J. Appl. Phys. **94**, 2680 (2003).